Axion Poltergeist

Keisuke Inomata

KICP, University of Chicago
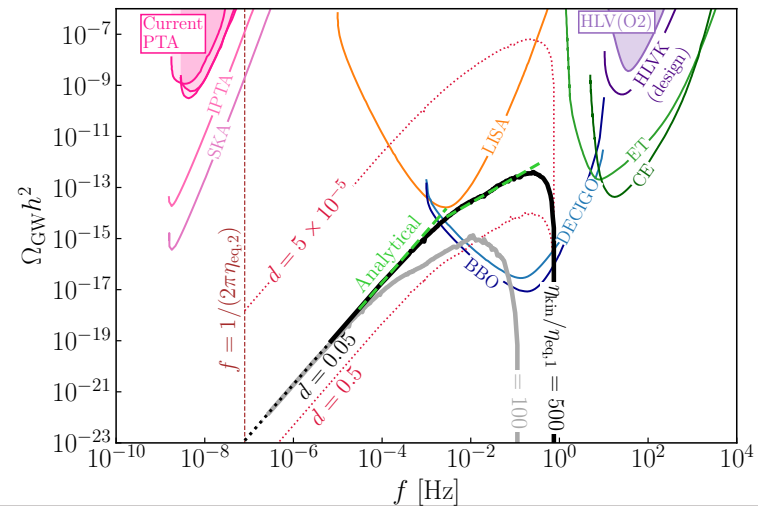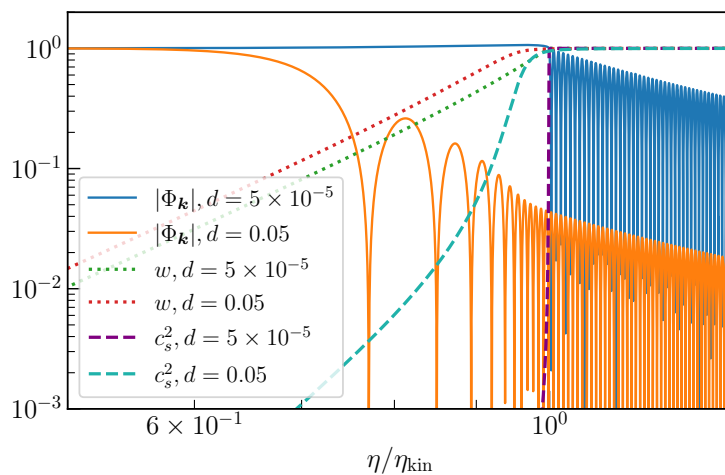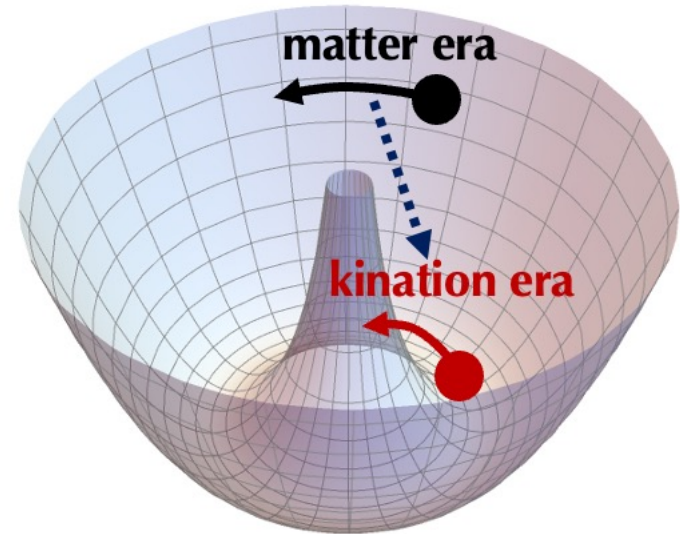
arXiv: 2305.14242

Collaborators:

Keisuke Harigaya (UChicago), Takahiro Terada (IBS, Korea)

Overview

We discuss the gravitational wave (GW) production through the **axion rotation.**

Strong GWs can be produced through the **Poltergeist mechanism** soon after the axion reaches the minimum.

Outline

- Background evolution with axion rotation
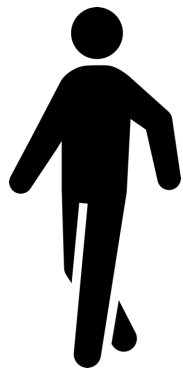- Perturbations and Poltergeist mechanism
- Summary

GWs as a probe of the early universe

GWs are not damped except for redshift once they are produced.

So, GWs are important footprints of the evolution of the early universe especially before big bang nucleosynthesis (BBN).

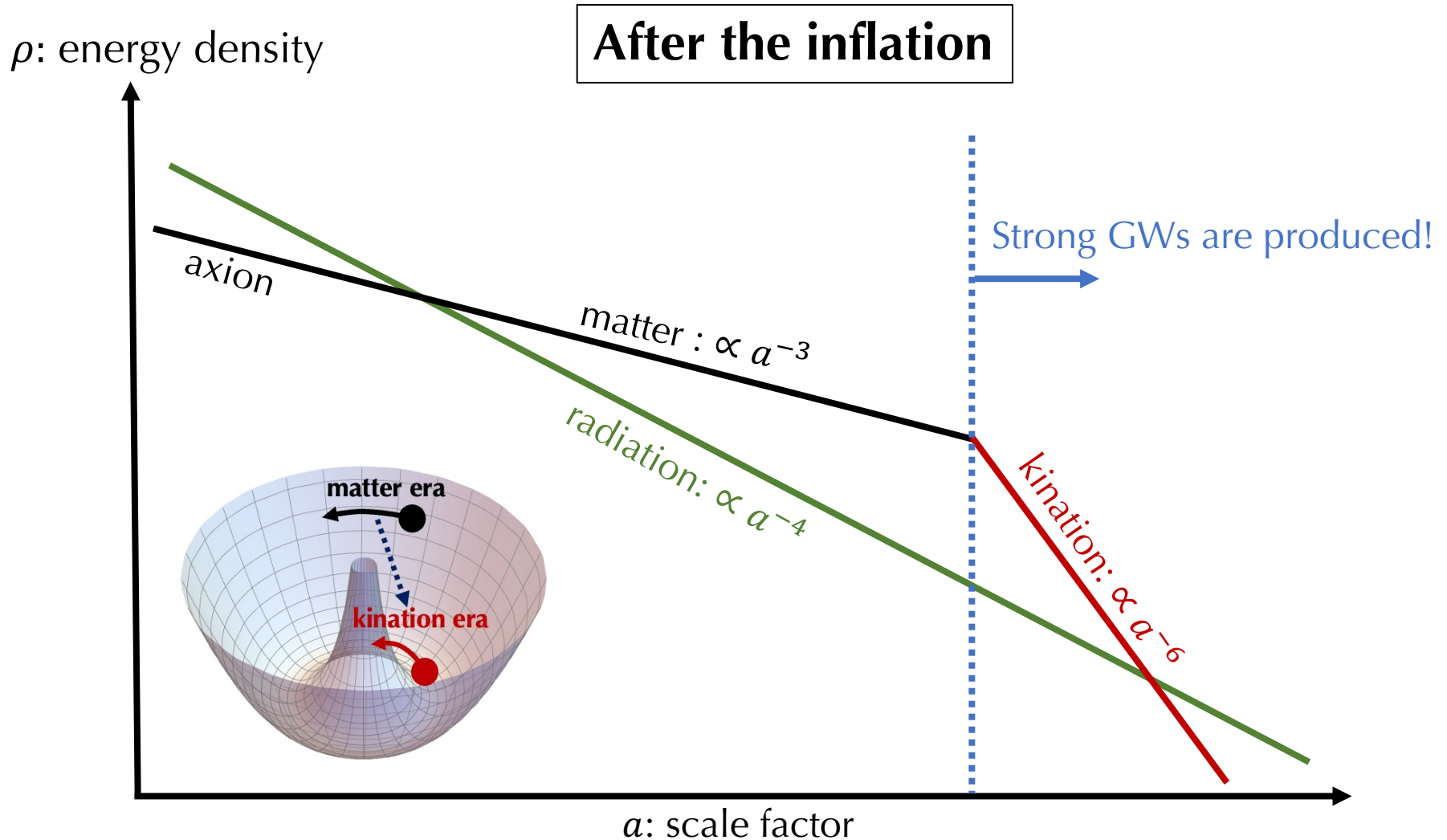In this work, we focus on GWs associated with transitions of different eras.

Current universe

CMB last scattering (T~O(0.1)eV)

BBN (T~O(1)MeV)

GW footprints that we focus on

Evolution of energy densities

ρ: energy density

After the inflation

a: scale factor

axion

matter : $\propto a^{-3}$

radiation: $\propto a^{-4}$

kination: $\propto a^{-6}$

Strong GWs are produced!

matter era

kination era

Axion rotation

We call the pseudo Nambu-Goldston boson associated with spontaneous breaking of U(1) symmetry "axion":

$$P = \frac{S}{\sqrt{2}} e^{ia/S}$$

P: complex scalar
a: axion
S: saxion

Initiation of axion rotation: (Co and Harigaya (2019))

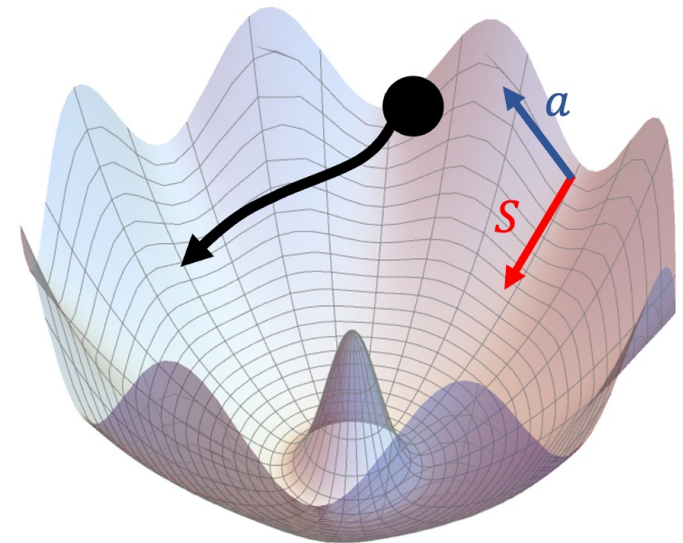**During the inflation**, $|P|$ becomes large e.g. due to the Hubble induced mass:

$$V(|P|) \sim -H^2|P|^2 + \frac{|P|^{2d}}{M^{2d-4}}$$

After the inflation, U(1) breaking higher order terms produce the angular momentum:

$$V(P) \sim \frac{P^n}{M^{n-4}} + \text{h.c.}$$

As $|P|$ decreases due to the Hubble expansion, the higher order terms become ineffective and the U(1) charge is fixed.

(Dynamics is similar to the Affleck-Dine baryogenesis. (Affleck, Dine 1985))

Fiducial model

Effective Lagrangian for Two-field model:

$$\mathcal{L} = \left(1 + \frac{f_a^4}{16|P|^4}\right)|\partial P|^2 - m_S^2\left(|P| - \frac{(1+d)f_a^2}{4|P|}\right)^2$$

$$= -\frac{r^4}{2(r^4 - 16v^4)}\partial^\mu r \partial_\mu r - \frac{r^2}{2}\partial^\mu\theta\partial_\mu\theta - V(r)$$

<u>canonicalized</u> $\left(2|P|^2\left(1 + \frac{v^4}{|P|^4}\right) = r^2, v = f_a/2\right)$

During the axion rotation,

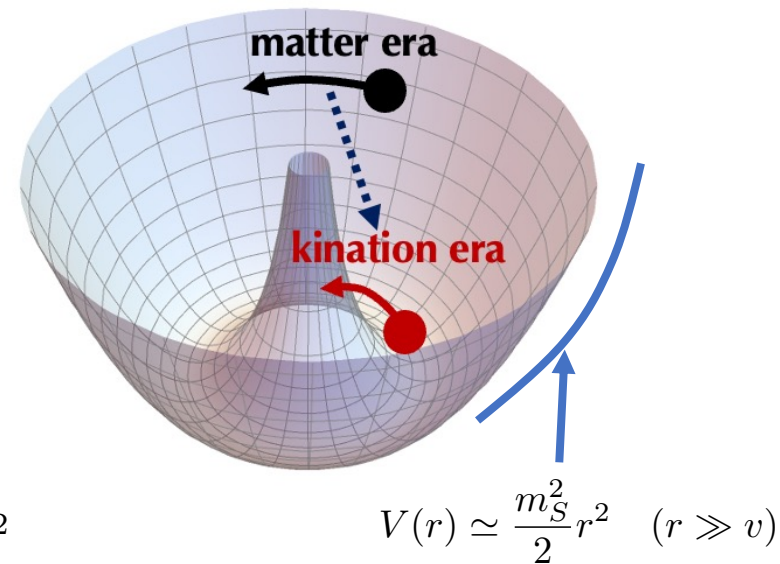$$w \equiv \frac{P}{\rho} \simeq \frac{\frac{r^2\dot{\theta}^2}{2} - V(r)}{\frac{r^2\dot{\theta}^2}{2} + V(r)}$$

Before the axion arrives at the minimum,
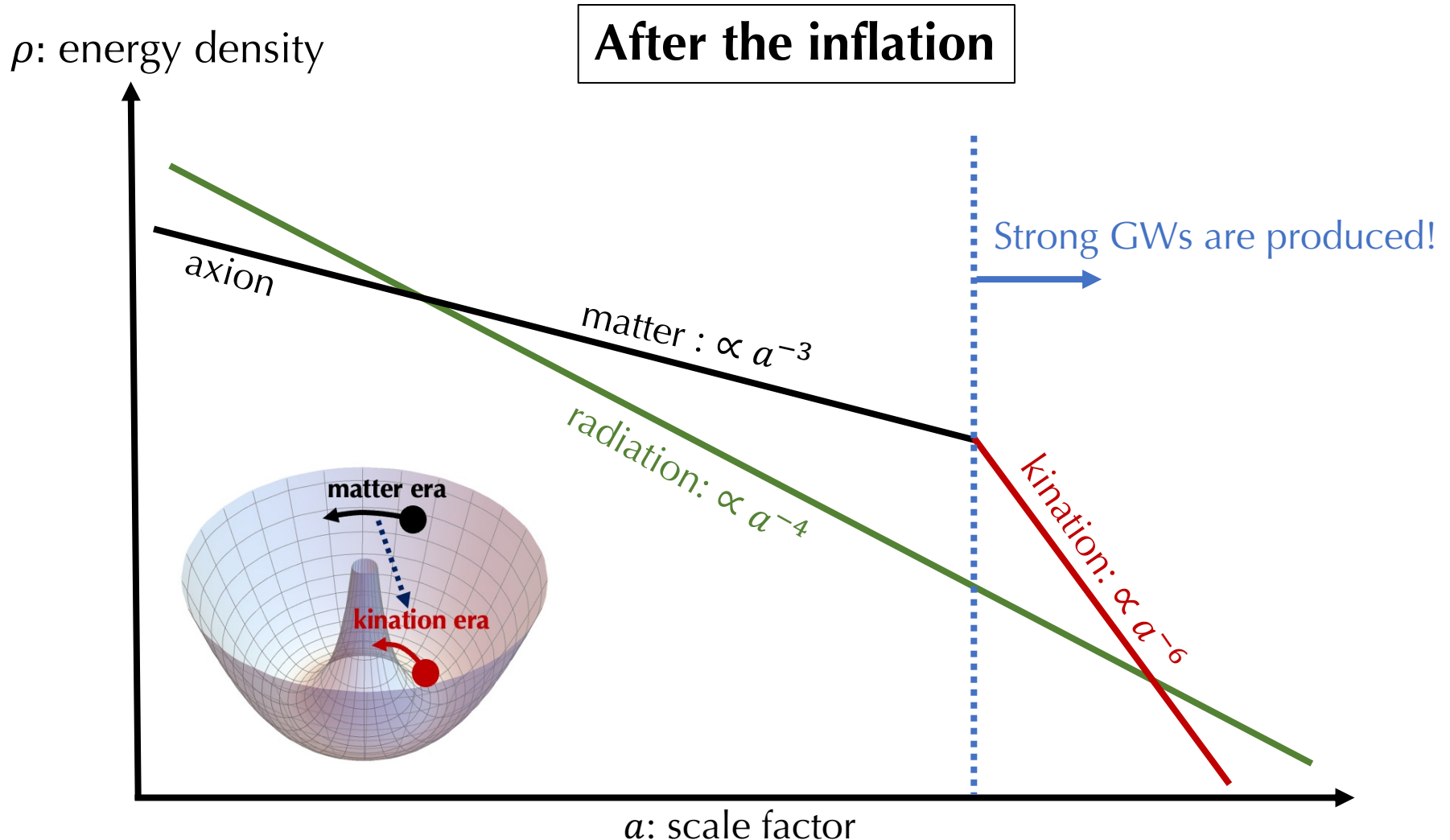The centripetal and centrifugal forces are balanced: $V' \simeq r\dot{\theta}^2$

$$\frac{r^2\dot{\theta}^2}{2} \simeq V(r) \rightarrow w \simeq 0 \text{ (MD)}$$

After the axion arrives at the minimum, the potential energy is negligible.

$$V(r) \ll \frac{r^2\dot{\theta}^2}{2} \rightarrow w \simeq 1 \text{ (KD)} \quad \text{(Spokoiny 1993, Joyce 1996)}$$

matter era

kination era

$$V(r) \simeq \frac{m_S^2}{2}r^2 \quad (r \gg v)$$

Evolution of energy densities

ρ: energy density

After the inflation

axion

matter : $\propto a^{-3}$

radiation: $\propto a^{-4}$

kination: $\propto a^{-6}$

Strong GWs are produced!

matter era

kination era

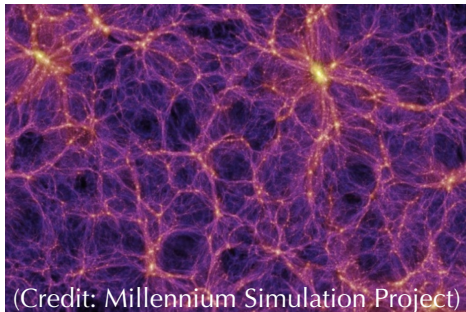a: scale factor

Outline

- Background evolution with axion rotation
- <u>Perturbations and Poltergeist mechanism</u>
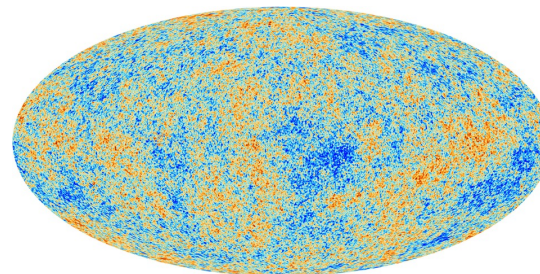- Summary

Scalar perturbations in Cosmology

Scalar perturbations are one of the most important quantities in Cosmology.

Scalar perturbations are origins of many things.

Examples

(Credit: Millennium Simulation Project)

Large Scale Structure

(Credit: ESA and the Planck Collaboration)

CMB anisotropies

From the observations, we already know the amplitude of the scalar perturbations.

$$\mathcal{P}_\zeta = 2.1 \times 10^{-9} \quad \text{(Planck 2018)}$$
$$(\delta\rho/\rho \sim 10^{-5})$$

Scalar perturbations originate from vacuum fluctuations of fields during the inflation era.

GWs induced by scalar perturbations

Metric perturbations:

Scalar perturbations (related to curvature perturbations)

$$ds^2 = a^2 \left[-(1 + 2\Phi)d\eta^2 + \left((1 - 2\Phi)\delta_{ij} + \frac{1}{2}h_{ij} \right) dx^i dx^j \right]$$

Tensor perturbations (GWs)

$$h^i_i = 0$$
$$\partial_i h^i_j = 0$$

Einstein equation:

$$G_{\mu\nu} = \frac{1}{M_{\rm Pl}^2} T_{\mu\nu}$$

$$G^i_j = a^{-2} \left[\frac{1}{4}(h^{i''}_j + 2\mathcal{H}h^{i'}_j - \Delta h^i_j) + 4\Phi\partial^i\partial_j\Phi + 2\partial^i\Phi\partial_j\Phi + A^i_j \right]$$

$$T^i_j = (\rho + P)\delta u^{,i}\delta u_{,j} + (P + \delta P)\delta^i_j$$

Terms irrelevant to tensor perturbations

E.o.m. for tensor perturbations:

$$h''_{ij} + 2\mathcal{H}h'_{ij} - \Delta h_{ij} = -4\hat{\mathcal{T}}_{ij}{}^{lm}\mathcal{S}_{lm}$$

$\hat{\mathcal{T}}_{ij}{}^{lm}$: Projection operator onto the transverse and traceless tensor

$$(w = P/\rho)$$

$$S_{ij} \simeq 4\Phi\partial_i\partial_j\Phi + 2\partial_i\Phi\partial_j\Phi - \frac{4}{3(1+w)\mathcal{H}^2}\partial_i(\Phi' + \mathcal{H}\Phi)\partial_j(\Phi' + \mathcal{H}\Phi)$$
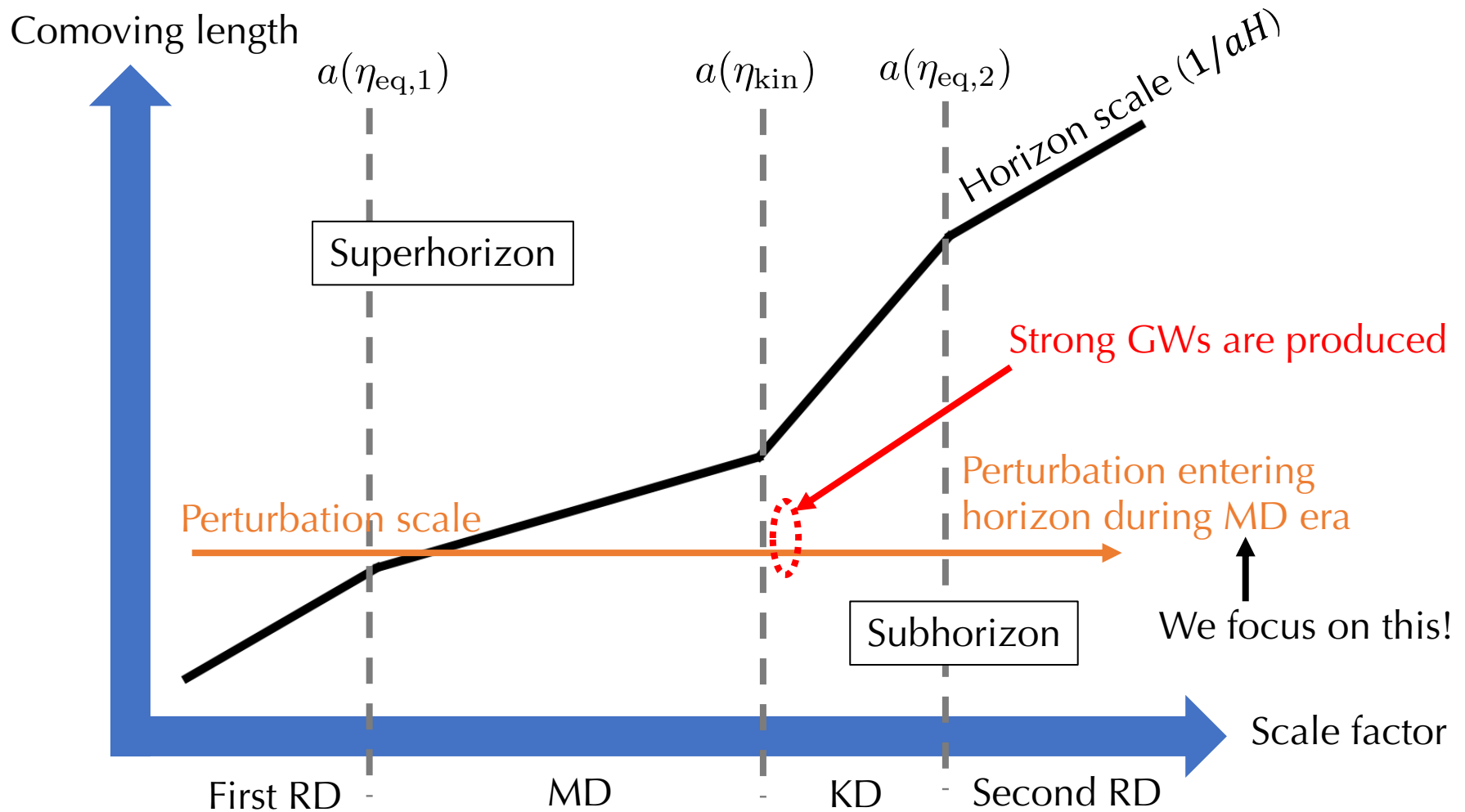
comes from $\delta u_{,i}\delta u_{,j}$ in T_{ij}

Point Scalar perturbations can induce GWs at second order. (Tomita 1967, Ananda et al. 2006, Baumann et al. 2007)
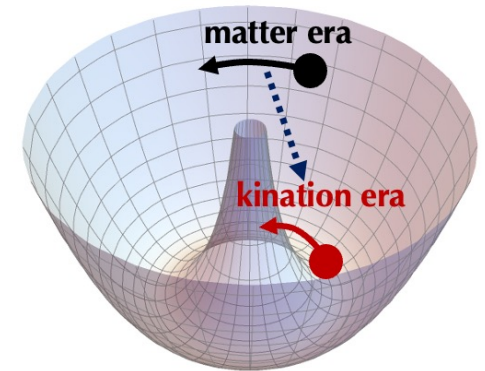
Evolution of scales
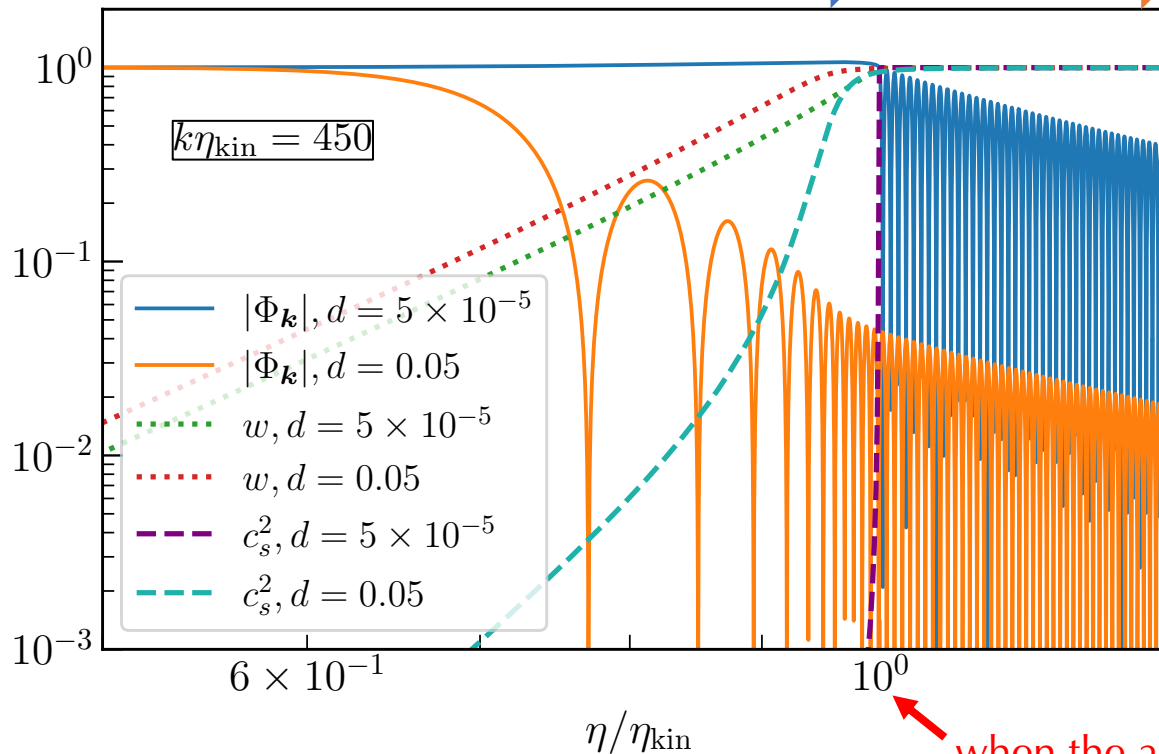

Comoving length

$a(\eta_{\mathrm{eq},1})$ $a(\eta_{\mathrm{kin}})$ $a(\eta_{\mathrm{eq},2})$

Horizon scale $(1/aH)$

Superhorizon

Strong GWs are produced

Perturbation scale

Perturbation entering horizon during MD era

Subhorizon

We focus on this!

Scale factor

First RD   MD   KD   Second RD

Evolution of scalar perturbations

$$\mathrm{d}s^2 = a^2 \left[-(1+2\Phi)\mathrm{d}\eta^2 + \left((1-2\Phi)\delta_{ij} + \frac{1}{2}h_{ij} \right) \mathrm{d}x^i \mathrm{d}x^j \right]$$

MD era ($w = 0$)   KD era ($w = 1$)

$$w = P/\rho$$

$k\eta_{\mathrm{kin}} = 450$

- $|\Phi_{\boldsymbol{k}}|, d = 5 \times 10^{-5}$
- $|\Phi_{\boldsymbol{k}}|, d = 0.05$
- $w, d = 5 \times 10^{-5}$
- $w, d = 0.05$
- $c_s^2, d = 5 \times 10^{-5}$
- $c_s^2, d = 0.05$

η/η_{kin}

matter era

kination era

when the axion reaches the minimum

Due to pressure, gravitational potential oscillates rapidly ($\sim 1/k$) during the KD era.

Poltergeist mechanism
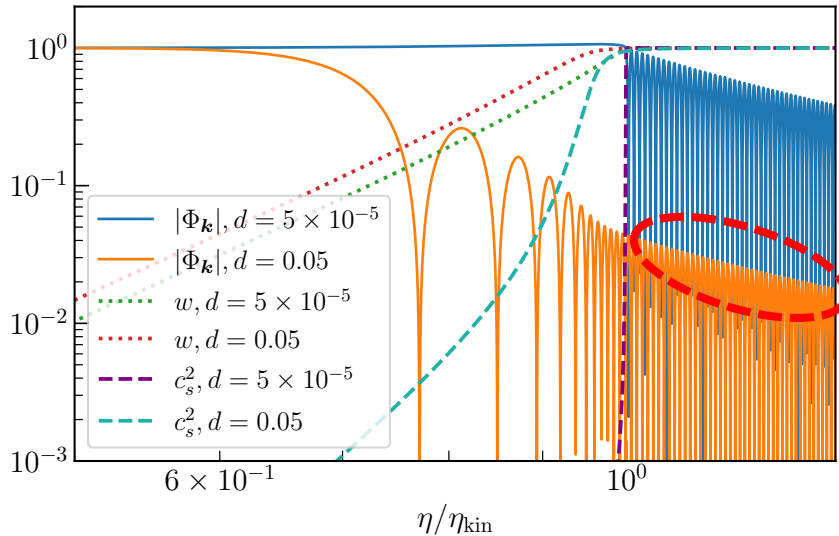
The fast oscillation is the main source for the GW production.

E.o.m. for tensor perturbations:

$$h_{ij}'' + 2\mathcal{H}h_{ij}' - \Delta h_{ij} = -4\hat{\mathcal{T}}_{ij}{}^{lm}\mathcal{S}_{lm}$$

$$S_{ij} \equiv 4\Phi\partial_i\partial_j\Phi + 2\partial_i\Phi\partial_j\Phi - \frac{4}{3(1+w)\mathcal{H}^2}\partial_i(\Phi'+\mathcal{H}\Phi)\partial_j(\Phi'+\mathcal{H}\Phi)$$

$$\mathcal{H}^{-2}(\Phi')^2 \sim (k\eta)^2\Phi^2$$
oscillation time scale is ~1/k

$$T_j^i = (\rho + P)\delta u^i \delta u_{,j} + (P + \delta P)\delta_j^i$$

➡ *kη* ≫ 1 for rapid oscillation

➡ Strong GWs are produced !
(Poltergeist mechanism)

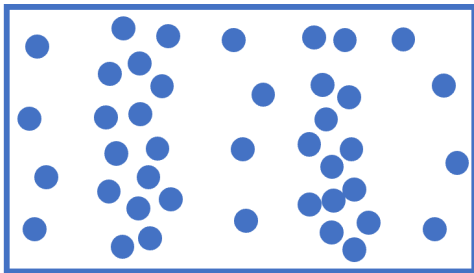**KI**, Kohri, Nakama, Terada, 2019
KI, Kawasaki, Mukaida, Terada, Yanagida, 2020
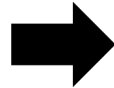
Why we call it "Poltergeist"?

"Poltergeist": German word for "noisy ghost" or "noisy spirit"

We first named it the "Poltergeist mechanism" in the context of sudden reheating.
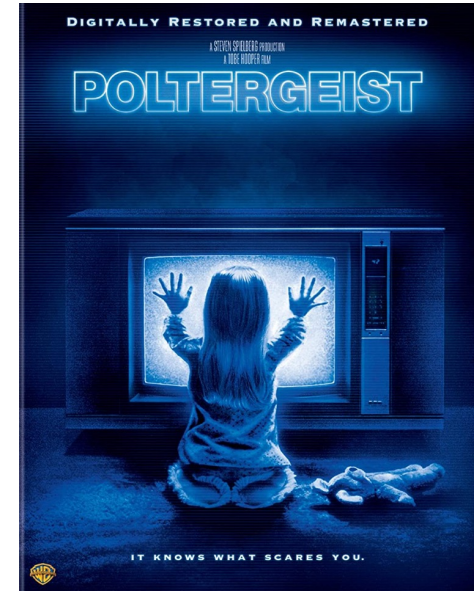
non-relativistic matter (or PBHs)
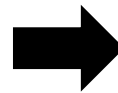
decay
(reheating)

radiation

(American supernatural horror film, 1982)

After the decay, "ghosts" of the non-relativistic matter "make a noise" in the thermal bath.

"ghosts" = produced radiation
"make a noise" = oscillation of sound wave
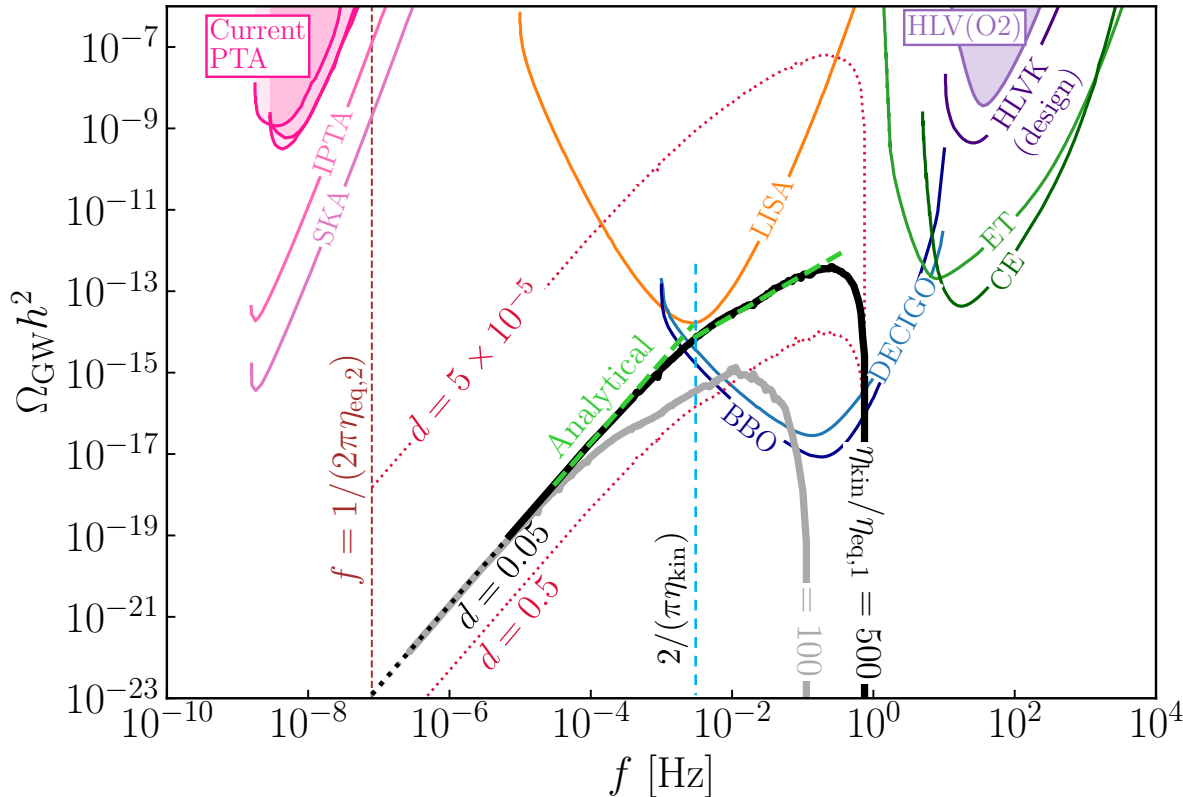
Strong GWs are produced !

KI, Kohri, Nakama, Terada, 2019
KI, Kawasaki, Mukaida, Terada, Yanagida, 2020

Related works that use this mechanism:

Domenech, Lin, Sasaki 2020 (PBH), Domenech, Takhistov, Sasaki 2021 (PBH), Bhaumik, Ghoshal, Jain, Lewicki 2022 (PBH)
White et al. 2021 (Q-ball), Kawasaki, Murai 2022 (Q-ball), Lozanov, Takhistov 2022 (Oscillon)

Gravitational wave spectrum


Smaller d corresponds to sharper transition.

The result for $d = 5 \times 10^{-5}$ is unreliable due to the strong coupling of the field fluctuations.

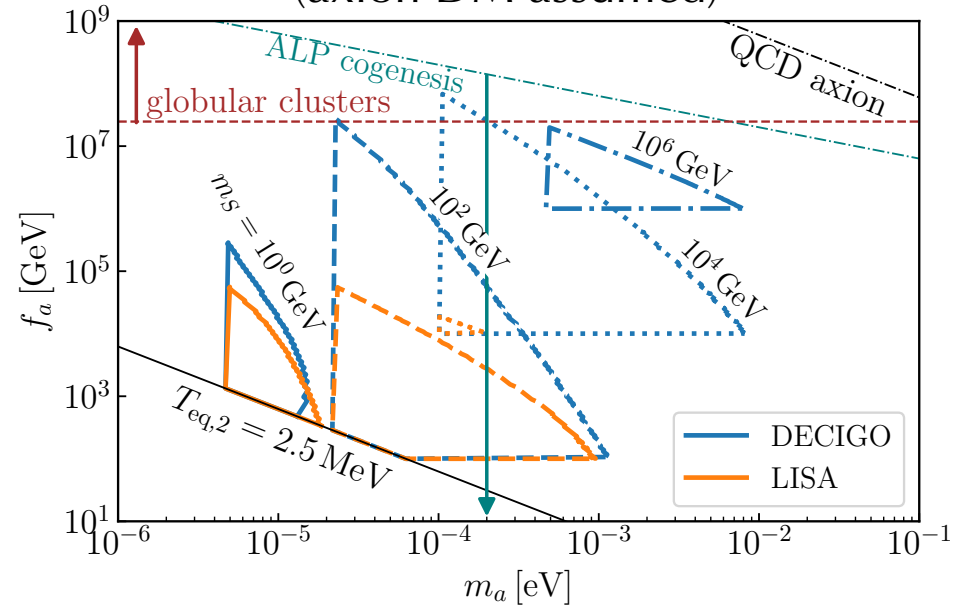$$\mathcal{P}_\zeta = 2.1 \times 10^{-9} \, \Theta(k_{\max} - k)\Theta(k - 1/\eta_{\mathrm{kin}})$$

small-scale cutoff
(very small-scale density perturbations become nonperturbative during MD)

horizon scale at the beginning of KD era
(superhorizon scale perturbations at that time are irrelevant to the Poltergeist mechanism.)
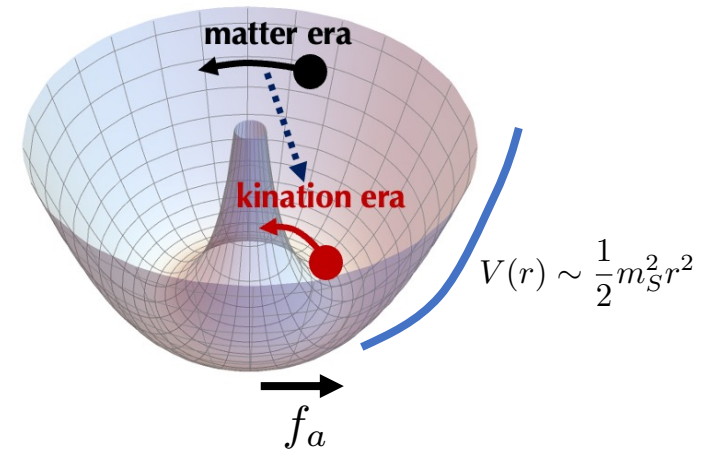
Observable parameter spaces
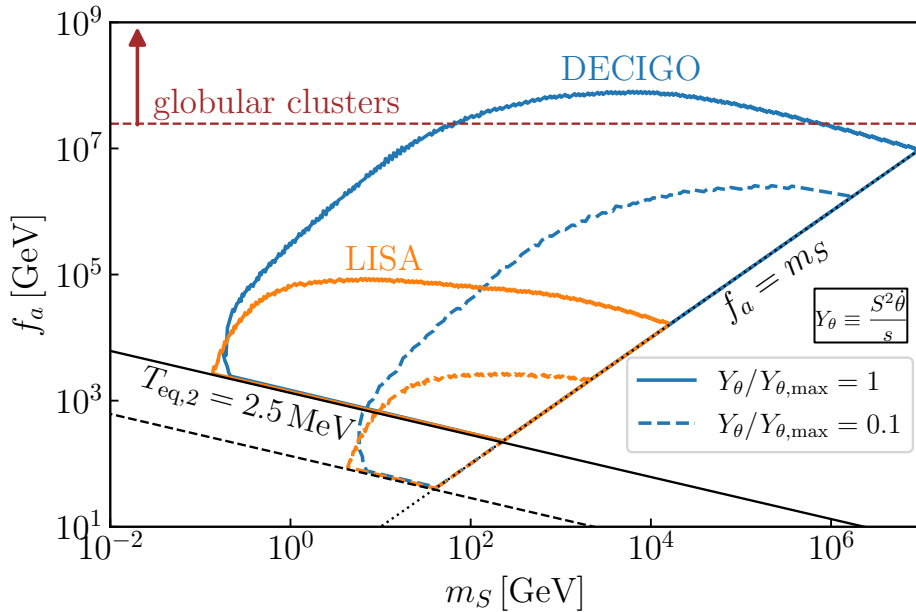
(axion DM assumed)

m_S corresponds to supersymmetry breaking scale in the two field model.

The future GW observations can probe the parameter regions even if there is no coupling between the axion and the standard model particles.
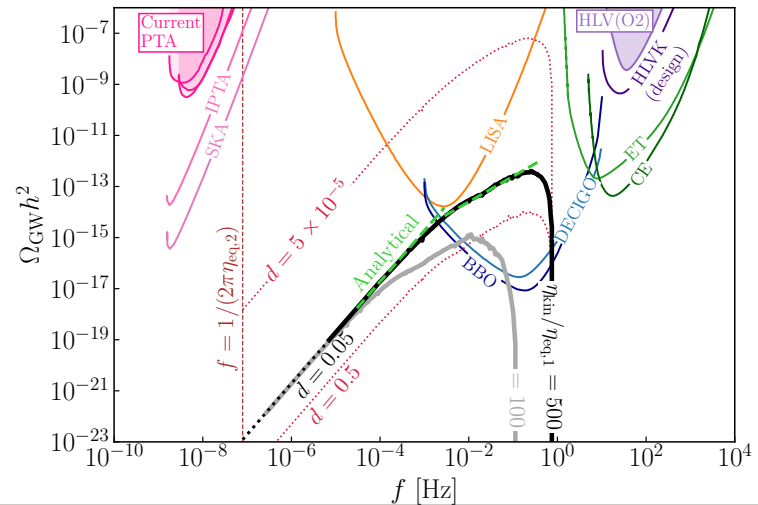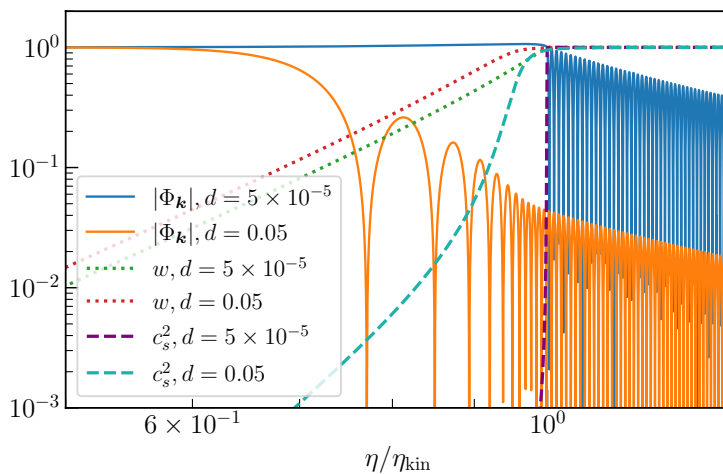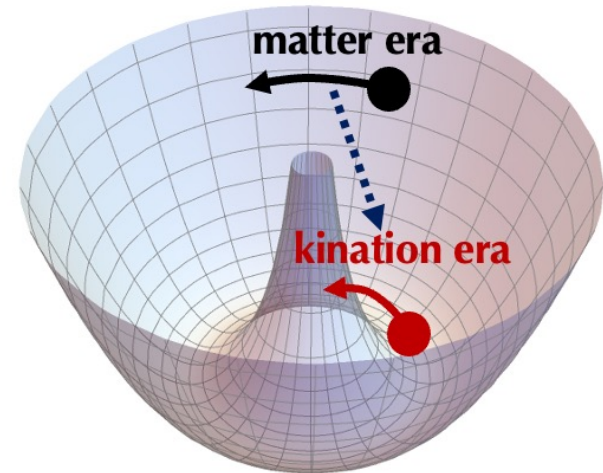

$$V(r) \sim \frac{1}{2} m_S^2 r^2$$

Outline

- Background evolution with axion rotation
- Perturbations and Poltergeist mechanism
- <u>Summary</u>

Summary

We discussed the gravitational wave (GW) production through the **axion rotation.**

Strong GWs can be produced through the **Poltergeist mechanism** soon after the axion reaches the minimum.

Backup

Limitation of linear analysis

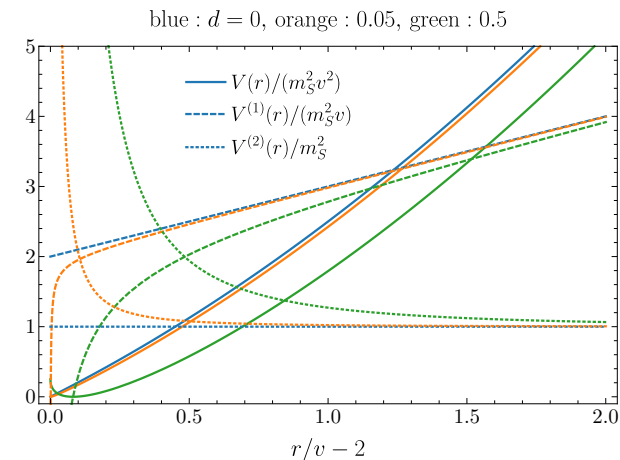There are limitations of the linear perturbation analysis.

1. Strong coupling of the radial field fluctuations.

$$\delta r'' + \cdots + V^{(2)} \delta r + \sum_{n=3} \frac{V^{(n)}}{(n-1)!} \delta r^{n-1} = 0$$

nonlinear contribution

Sharp feature enhances the higher derivative of potential.

Smaller d corresponds to a stronger coupling.

$d \gtrsim 0.05$ is in a weak coupling regime in our setup.

blue : $d = 0$, orange : 0.05, green : 0.5

Legend:
$V(r)/(m_S^2 v^2)$
$V^{(1)}(r)/(m_S^2 v)$
$V^{(2)}(r)/m_S^2$

x-axis: $r/v - 2$

2. Nonperturbative density perturbations.

During the MD era, the density perturbations grows $\propto a$ on subhorizon scales.

The small-scale density perturbations can be $\delta > 1$ at some point during MD era.

In our analysis, we introduce the small-scale cutoff for the curvature power spectrum.

Parameter relations

$$T_{\text{eq},1} \simeq 1.3 \times 10^8 \text{ GeV} \left(\frac{m_S}{10^5 \text{ GeV}} \right) \left(\frac{Y_\theta}{10^3} \right)$$

$$\boxed{Y_\theta \equiv \frac{S^2 \dot\theta}{s}}$$

$$T_{\text{kin}} \simeq 1.3 \times 10^4 \text{ GeV} \left(\frac{m_S}{10^5 \text{ GeV}} \right)^{1/3} \left(\frac{f_a}{10^6 \text{ GeV}} \right)^{2/3} \left(\frac{10^3}{Y_\theta} \right)^{1/3}$$

$$T_{\text{eq},2} = 1.8 \times 10^2 \text{ GeV} \times \left(\frac{f_a}{10^6 \text{ GeV}} \right) \left(\frac{Y_\theta}{10^3} \right)^{-1}$$

$$T_{\text{kin}}^3 \sim T_{\text{eq},1} T_{\text{eq},2}^2$$

$$\frac{1}{2\pi\eta_{\text{eq},2}} = 1.1 \times 10^{-5} \text{ Hz} \times \left(\frac{T_{\text{eq},2}}{1.8 \times 10^2 \text{ GeV}} \right)$$

$$\frac{\eta_{\text{kin}}}{\eta_{\text{eq},1}} = 1.7 \times 10^2 \left(\frac{m_S}{10^5 \text{ GeV}} \right)^{\frac{1}{3}} \left(\frac{f_a}{10^6 \text{ GeV}} \right)^{-\frac{1}{3}} \left(\frac{Y_\theta}{10^3} \right)^{\frac{2}{3}}$$

$$Y_{\theta,\text{max}} = 10^3 \left(\frac{m_S}{8.7 \times 10^5 \text{ GeV}} \right)^{-\frac{1}{3}} \left(\frac{b}{0.1} \right)^{\frac{1}{3}}$$

UV completion of fiducial model

Supersymmetric UV completion of the fiducial model:

$$K = |P|^2 + |\bar{P}|^2 + |X|^2$$
$$W = \lambda X(P\bar{P} - v^2)$$
$$V = \lambda^2|P\bar{P} - v^2|^2 + \lambda^2|X|^2(|P|^2 + |\bar{P}|^2)$$

$\bar{P}P = v^2$ is the flat direction.
In addition, we consider the soft SUSY breaking term:

$$V_{\text{soft}} = m_P^2|P|^2 + m_{\bar{P}}^2|\bar{P}|^2$$

We can consider $|P| \gg |\bar{P}|$ without loss of generality and integrate out $\bar{P}$, which leads to $\bar{P} \simeq \frac{v^2}{P}$.

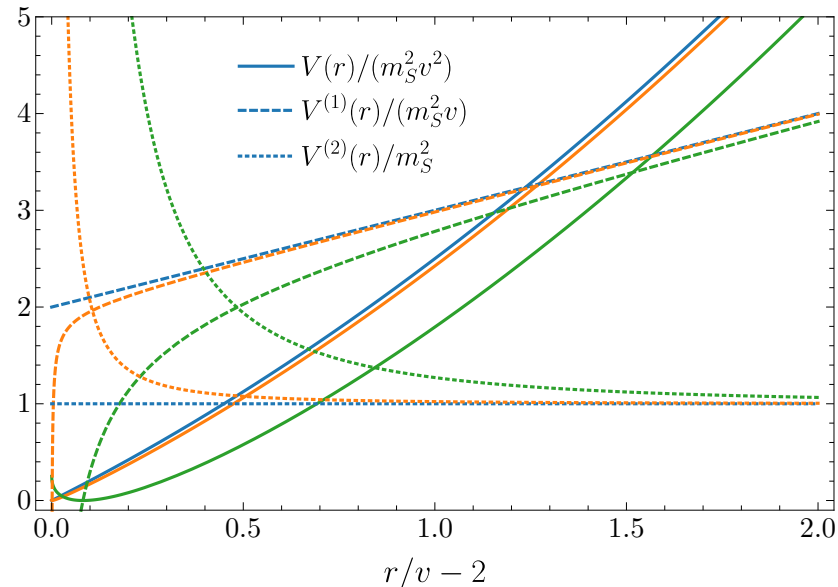Substituting $\bar{P} \simeq \frac{v^2}{P}$ to the Lagrangian, we obtain

$$\mathcal{L} = \left(1 + \frac{f_a^4}{16|P|^4}\right)|\partial P|^2 - m_S^2\left(|P| - \frac{(1+d)f_a^2}{4|P|}\right)^2$$

$$(m_S = m_P, 1 + d = m_{\bar{P}}/m_P, f_a = 2v)$$

Potential in two-field model

$$\mathcal{L} = \left(1 + \frac{f_a^4}{16|P|^4}\right)|\partial P|^2 - m_S^2\left(|P| - \frac{(1+d)f_a^2}{4|P|}\right)^2$$

$$= -\frac{r^4}{2(r^4 - 16v^4)}\partial^\mu r \partial_\mu r - \frac{r^2}{2}\partial^\mu\theta\partial_\mu\theta$$

$$- \frac{1}{4}m_S^2\left(\sqrt{r^2 + \sqrt{r^4 - 16v^4}} - \frac{4(1+d)v^2}{\sqrt{r^2 + \sqrt{r^4 - 16v^4}}}\right)^2$$

blue : $d = 0$, orange : 0.05, green : 0.5

Potential in two-field model in S

$$\mathcal{L} = \left(1 + \frac{f_a^4}{16|P|^4}\right)|\partial P|^2 - m_S^2\left(|P| - \frac{(1+d)f_a^2}{4|P|}\right)^2$$

$$= -\frac{r^4}{2(r^4 - 16v^4)}\partial^\mu r \partial_\mu r - \frac{r^2}{2}\partial^\mu\theta\partial_\mu\theta$$

$$\quad - \frac{1}{4}m_S^2\left(\sqrt{r^2 + \sqrt{r^4 - 16v^4}} - \frac{4(1+d)v^2}{\sqrt{r^2 + \sqrt{r^4 - 16v^4}}}\right)^2$$

$$= -\frac{\chi(S)}{2}(\partial^\mu S\partial_\mu S + S^2\partial^\mu\theta\partial_\mu\theta) - \frac{m_S^2}{2}\left(S - \frac{2(1+d)v^2}{S}\right)^2 \quad \chi(S) = 1 + 4v^4/S^4$$

The balance of the centripetal and centrifugal force:

$$V'(r) \simeq r\dot{\theta}^2 \rightarrow V'(S) \simeq \underline{(\chi(S)S^2)_{,S}}\dot{\theta}^2$$

This goes approaches zero at $S \neq 0$.

The decrease of the centrifugal force

The roll down gets accelerated

Thermalization

The orbit is initially elliptical, but the thermalization changes it to the circular orbit.

For the elliptical orbit, the evolution of $|P|$ can be divided into two: fast oscillating mode and (relatively) slowly evolving mode
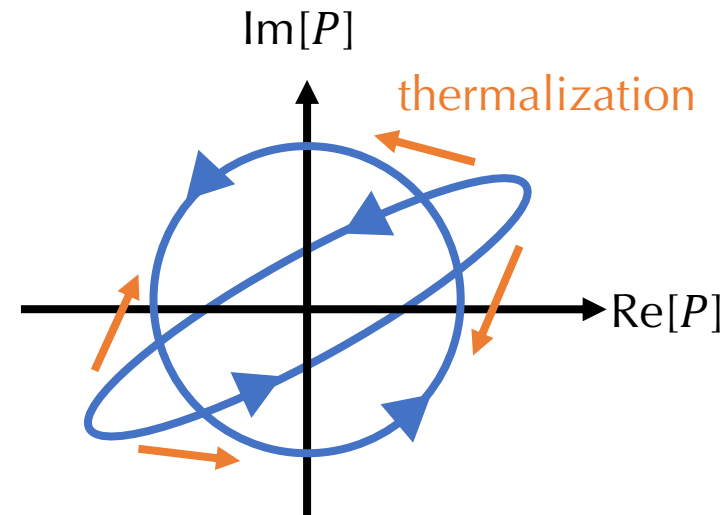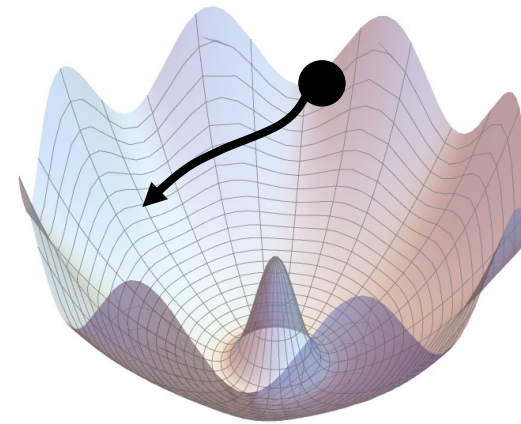
$$|P| = \hat{P}^{\text{fast}} + \hat{P}^{\text{slow}}$$

$$\dot{\hat{P}}^{\text{fast}} \sim m_S \hat{P}^{\text{fast}}, \quad \dot{\hat{P}}^{\text{slow}} \sim H \hat{P}^{\text{slow}}$$

This makes the orbit elliptical

$\hat{P}^{\text{fast}}$ is not protected by the U(1) charge conservation and therefore they can be easily dissipated to thermal bath through some interaction (thermalization).

➡ The orbit finally becomes circular.

Additional Enhancement from redshift

Once gravitational waves are produced, they behave as radiation, whose energy density is $\rho_{GW} \propto a^{-4}$.
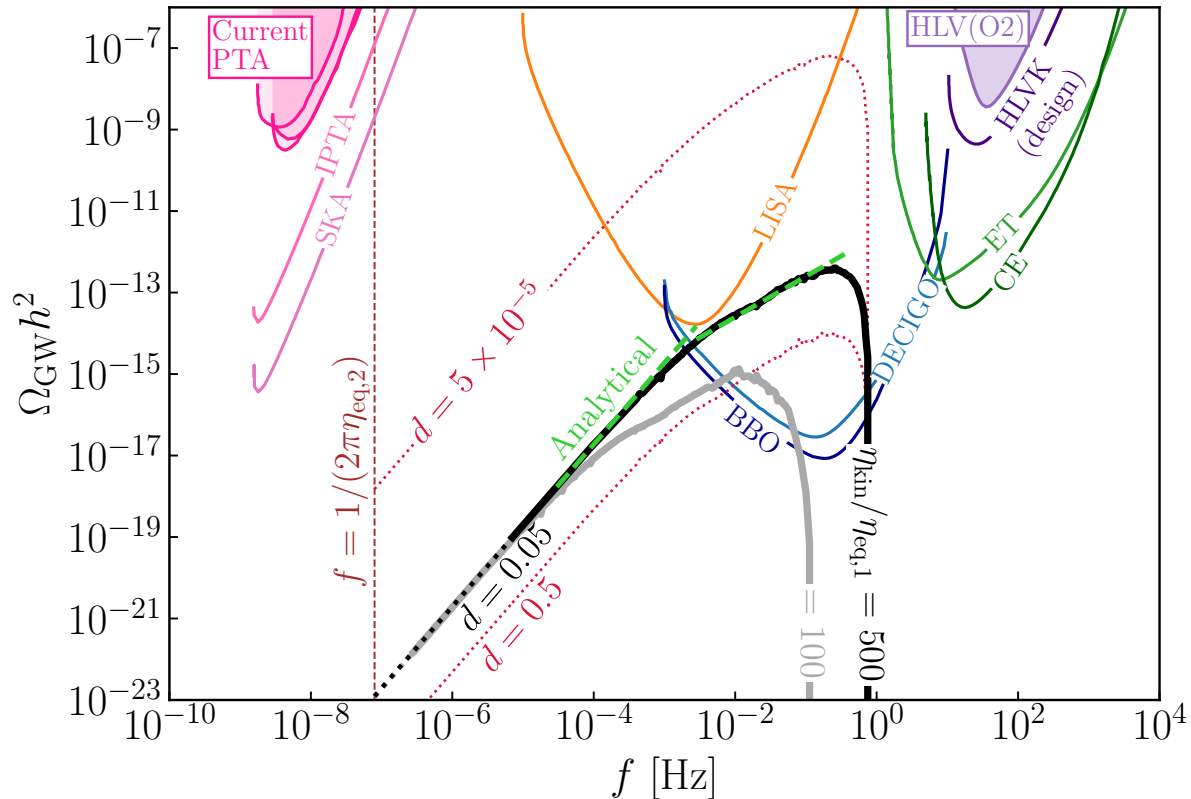
On the other hand, the total energy density during the KD era is $\rho_{tot} \propto a^{-6}$.

Then, we find

$$\Omega_{\text{GW}} \equiv \frac{\rho_{\text{GW}}}{\rho_{\text{tot}}} \propto a^2 \quad (\text{during KD})$$

The GWs produced around the beginning of KD era get enhanced by $\frac{a(\eta_{eq,2})^2}{a(\eta_{kin})^2} \sim \frac{\eta_{eq,2}}{\eta_{kin}}$, in addition to the enhancement of the Poltergeist mechanism.
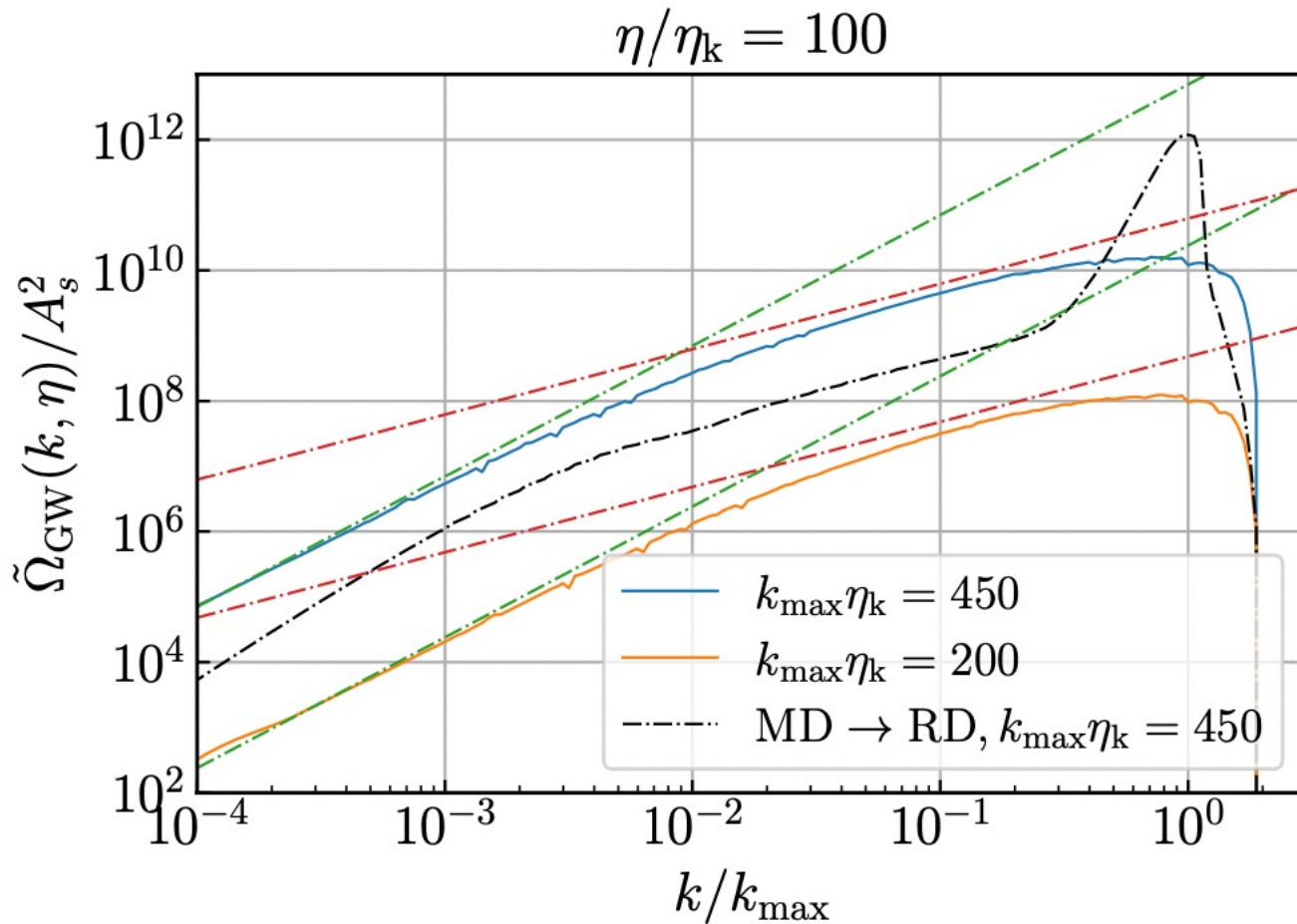
Analytical formula

$$\mathcal{P}_\zeta = A\,\Theta(k_{\max} - k)\Theta(k - 1/\eta_{\mathrm{kin}}) \qquad k_* = \max[k_{\max}, 1/\eta_{\mathrm{eq},1}]$$

$$\Omega_{\mathrm{GW}}h^2 \simeq 2 \times 10^{-11} A^2 Q^4 B(k)\,\frac{\eta_{\mathrm{kin}}^2}{\eta_{\mathrm{eq},1}^2}\,k_*^5 k \eta_{\mathrm{kin}}^6$$

Comparison of GW spectrum

DECIGO (2006.13545)

Abstract: Deci-hertz Interferometer Gravitational Wave Observatory (DECIGO) is the future mission that aims to detect gravitational waves between 0.1 Hz and 10 Hz. DECIGO has four clusters, and one cluster of DECIGO consists of three differential Fabry-Perot interferometers with three drag-free spacecraft. Among various science targets of DECIGO, the detection of primordial gravitational waves is crucial. We are now updating the DECIGO design to ensure the detection of the primordial gravitational waves. We aim to launch B-DECIGO first at the earliest in 2032 as a pathfinder mission of DECIGO. B-DECIGO will not only establish the necessary technologies for DECIGO, but also accomplish a variety of important sciences.
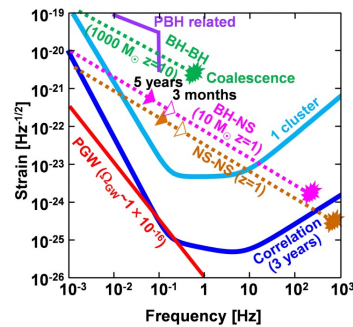
Fig. 3. Target sensitivity of DECIGO and expected gravitational wave signals.
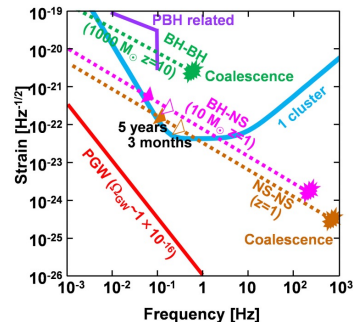

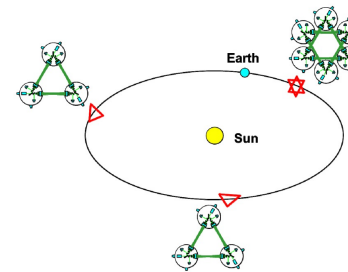Fig. 5. Target sensitivity of B-DECIGO and expected gravitational wave signals.

Fig. 1. Orbit of DECIGO. Four clusters of DECIGO are put in the heliocentric orbit: two at the same position and the other two at different positions.
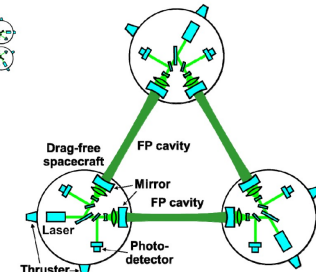
Fig. 2. Conceptual design of DECIGO. One cluster of DECIGO consists of three drag-free spacecraft. FP cavities are used to measure a change in the arm length.

Table 1. Optical and mechanical parameters of DECIGO and B-DECIGO [10].

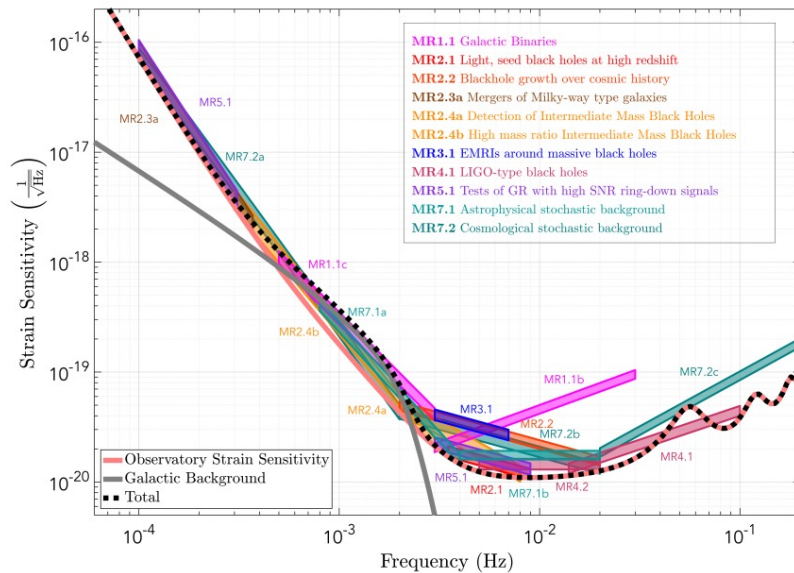| Optical/mechanical parameter	DECIGO	B-DECIGO
Arm length (km)	1,000	100
Laser power (W)	10	1
Laser wavelength (nm)	515	515
Finesse	10	100
Mirror diameter (m)	1	0.3
Mirror mass (kg)	100	30
# of clusters	4	1
# of interferometers per cluster	3	3

LISA

Figure 2: Mission constraints on the sky-averaged strain sensitivity of the observatory for a 2-arm configuration (TDI X), $\sqrt{S_h(f)}$, derived from the threshold systems of each observational requirement.
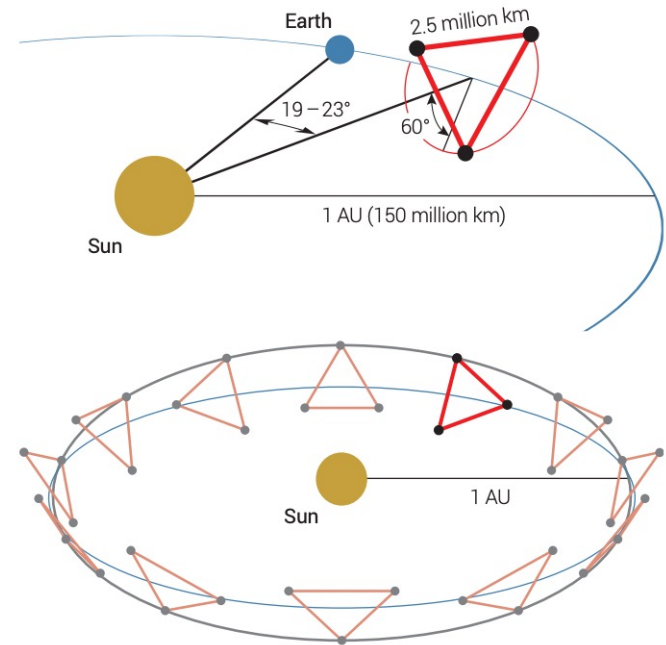

Figure 4: Depiction of the LISA Orbit.

(from 1702.00786)

Launch in Mid-2030s
(The 14th International LISA Symposium, July in 2022)